Synthesis, Structure, and Bridge-Terminal Exchange Kinetics of Pyrazolate-Bridged Digallium and Diindium Complexes Containing Bridging Phenyl Groups

Chatu T. Sirimanne, Wenjun Zheng, Zhengkun Yu, Mary Jane Heeg, and Charles H. Winter*

Department of Chemistry, Wayne State University, Detroit, Michigan 48202

Received July 25, 2005

Treatment of triphenylgallium with 3,5-dimethylpyrazole, 3,5-diphenylpyrazole, or 3,5-di-*tert*-butylpyrazole in a 2:1 stoichiometry afforded the phenyl-bridged complexes $(C_6H_5)_2Ga(\mu\text{-}Me_2pz)(\mu\text{-}C_6H_5)Ga(C_6H_5)_2$ (62%), $(C_6H_5)_2Ga(\mu\text{-}Ph_2pz)(\mu\text{-}C_6H_5)Ga(C_6H_5)_2\cdot C_7H_8$ (62%), and $(C_6H_5)_2Ga(\mu\text{-}tBu_2pz)(\mu\text{-}C_6H_5)Ga(C_6H_5)_2$ (40%), respectively, as colorless or off-white crystalline solids. Treatment of triphenylindium with 3,5-di-*tert*-butylpyrazole in a 2:1 stoichiometry afforded the phenyl-bridged complex $(C_6H_5)_2In(\mu\text{-}tBu_2pz)(\mu\text{-}C_6H_5)In(C_6H_5)_2\cdot(C_6H_{14})_{0.5}$ (40%). The molecular structures of $(C_6H_5)_2Ga(\mu\text{-}Ph_2pz)(\mu\text{-}C_6H_5)Ga(C_6H_5)_2\cdot C_7H_8$, $(C_6H_5)_2Ga(\mu\text{-}tBu_2pz)(\mu\text{-}C_6H_5)Ga(C_6H_5)_2\cdot(C_6H_{14})_{0.5}$, and $(C_6H_5)_2In(\mu\text{-}tBu_2pz)(\mu\text{-}C_6H_5)In(C_6H_5)_2\cdot(C_6H_{14})_{0.5}$ consist of a 3,5-disubstituted pyrazolato ligand with a diphenylgallio or diphenylindio group bonded to each nitrogen atom. A phenyl group acts as a bridge between the two metal atoms. By contrast, treatment of triphenylgallium with 3,5-di-*tert*-butylpyrazole in a 1:1 stoichiometry or triphenylindium with 3,5-diphenylpyrazole or 3,5-dimethylpyrazole in 2:1 or 1:1 stoichiometry afforded the dimeric complexes $[(C_6H_5)_2Ga(\mu\text{-}tBu_2pz)]_2$ (63%), $[(C_6H_5)_2In(\mu\text{-}Ph_2pz)]_2$ (40%), and $[(C_6H_5)_2In(\mu\text{-}Me_2pz)]_2$ (92%), respectively, as colorless crystalline solids. The dimeric nature of these complexes was determined by X-ray crystallography. Treatment of 3,5-di-*tert*-butylpyrazole with excess trimethylgallium afforded the dimeric complex $[Me_2Ga(\mu\text{-}tBu_2pz)]_2$ (82%) as the major product and $Me_2Ga(\mu\text{-}tBu_2pz)(\mu\text{-}OCH_3)GaMe_2$ (2.6%) as a minor product. There was no evidence for the formation of the methyl-bridged complex $Me_2Ga(\mu\text{-}tBu_2pz)(\mu\text{-}CH_3)GaMe_2$. The kinetics of bridge-terminal phenyl exchange in $(C_6H_5)_2Ga(\mu\text{-}Me_2pz)(\mu\text{-}C_6H_5)Ga(C_6H_5)_2$, $(C_6H_5)_2Ga(\mu\text{-}Ph_2pz)(\mu\text{-}C_6H_5)Ga(C_6H_5)_2\cdot C_7H_8$, $(C_6H_5)_2Ga(\mu\text{-}tBu_2pz)(\mu\text{-}C_6H_5)Ga(C_6H_5)_2$, and $(C_6H_5)_2In(\mu\text{-}tBu_2pz)(\mu\text{-}C_6H_5)In(C_6H_5)_2\cdot(C_6H_{14})_{0.5}$ was determined by ^{13}C NMR spectroscopy and afforded the following range of activation parameters: $\Delta H^{\ddagger} = 6.0-8.9$ kcal/mol, $\Delta S^{\ddagger} = -23.1$ to -32.0 eu, and $\Delta G^{\ddagger}_{(298\ K)} = 15.5-15.8$ kcal/mol. The large, negative values of $\Delta S^{\ddagger}$ imply ordered transition states relative to the ground state and rotation along the $N-GaPh_3$ or $N-InPh_3$ vector without metal−nitrogen bond cleavage. The combined results suggest that the close proximity of the metal atoms is the principal determinant of the bridging phenyl interactions and that complexes of the heavier group 13 elements with bridging hydrocarbon ligands are likely to be more accessible than the current state of literature would suggest.

Introduction

The bridging of monoanionic hydrocarbon groups such as alkyl,[1,2] aryl,[3] acetylide,[4] and alkenyl[4] between two metal centers is well established for the lighter main group elements and is particularly broadly appreciated for aluminum. Classic aluminum complexes with bridging hydrocarbon ligands include dimeric trimethylaluminum[1] and dimeric triphenylaluminum.[3a] Despite the broad occurrence of bridging interactions in aluminum chemistry, there are very few examples of similar bridging hydrocarbon ligands between the heavier group 13 elements gallium and indium. Structurally characterized examples for gallium are limited to $[Me_2Ga(\mu\text{-}CCPh)]_2$[5a] and a gallole dimer containing bridging alkenyl groups.[5b] For indium, the only example is $[Me_2In(\mu\text{-}2\text{-}C_4H_3S)]_2$.[6] Several classes of cyclopentadienyl complexes also contain formal cyclopentadienyl bridges between gallium or indium and other metal centers.[7,8] A small number of gallium-substituted ferrocenes have been structurally characterized.[7] Indium(I) cyclopentadienyl complexes contain various bridging cyclopentadienyl ligands.[8] In addition, a few group 13 heteronuclear complexes have been structurally documented in which a mesityl group bridges between boron and gallium or boron and indium,[9] and an alkenyl group bridges between boron and indium.[10]

Some striking differences exist between aluminum and gallium complexes containing similar hydrocarbon

(1) Crystal structure determinations of dimeric trimethylaluminum: (a) Huffman, J. C.; Streib, W. E. *Chem. Commun.* **1971**, 911. (b) Byram, S. K.; Fawcett, J. K.; Nyburg, S. C.; O'Brien, R. J. *Chem. Commun*. **1970**, 16. (c) Vranka, R. G.; Amma, E. L. *J. Am. Chem. Soc.* **1967**, *89*, 3121. (d) Lewis, P. H.; Rundle, R. E. *J. Chem. Phys.* **1953**, *21*, 986. (e) Evans, W. J.; Anwander, R.; Ziller, J. W. *Organometallics* **1995**, *14*, 1107.

10.1021/om050623r CCC: $30.25
Publication on Web 11/04/2005

ligands. For example, triphenylaluminum is dimeric in the solid state with two bridging phenyl groups,[3a] while triphenylgallium and triphenylindium are monomeric in the solid state and have only long, weak intermolecular contacts between the metal atoms and phenyl ligand carbon atoms.[11] Trimethylaluminum is dimeric in the solid state and in solution with a well-known methyl-bridged structure,[1] while the methyl groups in solid trimethylgallium have only very weak bridge-like interactions between neighboring gallium atoms.[12a,b]

Within this perspective, we report the synthesis, structural characterization, and bridge-terminal exchange kinetics of a series of gallium and indium pyrazolato complexes that contain bridging phenyl ligands. The observation of bridging phenyl ligands in these complexes is particularly surprising, since triphenylgallium and triphenylindium are monomeric. The results imply that bridging interactions in the heavier elements may be induced by appropriate choice of ancillary ligands that dispose two metal centers in close proximity. Thus, complexes of the heavier group 13 elements with bridging hydrocarbon ligands are likely to be more accessible than the current literature may suggest. We also describe attempts to prepare a bridging methyl complex of gallium. A portion of this work was communicated.[13]

Results

Synthesis of Phenyl-Bridged Gallium and Indium Pyrazolato Complexes. Treatment of triphenylgallium (2 equiv) with 3,5-dimethylpyrazole, 3,5-diphenylpyrazole, or 3,5-di-*tert*-butylpyrazole afforded $(C_6H_5)_2Ga(\mu\text{-}Me_2pz)(\mu\text{-}C_6H_5)Ga(C_6H_5)_2$ (**1**, 62%), $(C_6H_5)_2Ga(\mu\text{-}Ph_2pz)(\mu\text{-}C_6H_5)Ga(C_6H_5)_2\cdot C_7H_8$ (**2**·C_7H_8, 62%), and $(C_6H_5)_2Ga(\mu\text{-}tBu_2pz)(\mu\text{-}C_6H_5)Ga(C_6H_5)_2$ (**3**, 40%), respectively, as colorless or off-white crystalline solids (eq 1). Similar treatment of triphenylindium with 3,5-di-*tert*-butylpyrazole afforded $(C_6H_5)_2In(\mu\text{-}tBu_2pz)(\mu\text{-}C_6H_5)In(C_6H_5)_2\cdot(C_6H_{14})_{0.5}$ (**4**·$(C_6H_{14})_{0.5}$, 40%) as colorless crystals. The structural assignments for **1**, **2**·C_7H_8, **3**, and **4**·$(C_6H_{14})_{0.5}$ were based on spectral and analytical data and X-ray crystal structure determinations. The ^1H NMR spectra of **1**, **2**·C_7H_8, and **3** at ambient temperature showed three broad multiplets for the bridging phenyl groups and sharper multiplets for the terminal phenyl groups. The $^{13}C\{^1H\}$ NMR spectra at ambient temperature exhibit broad *ipso*-carbon resonances for the bridging and terminal phenyl rings in the range 157.33−158.33 and 146.45−148.26 ppm, respectively. In the NMR spectra of **4**·$(C_6H_{14})_{0.5}$ at ambient temperature, broad resonances for one type of phenyl ligand were observed, which suggested that the coalescence temperature for phenyl site exchange was below ambient temperature.

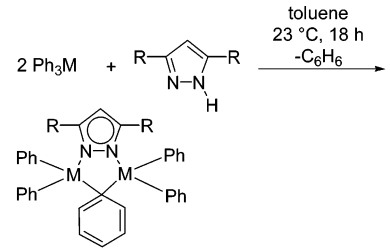

(1)

1, M = Ga, R = Me, 62%
2·C_7H_8, M = Ga, R = Ph, 62%
3, M = Ga, R = tBu, 40%
4·$(C_6H_{14})_{0.5}$, M = In, R = tBu, 40%

(2) Recent selected reports of structurally characterized aluminum complexes with bridging alkyl ligands: (a) Son, A. J. R.; Thorn, M. G.; Fanwick, P. E.; Rothwell, I. P. *Organometallics* **2003**, *22*, 2318. (b) Hair, G. S.; Cowley, A. H.; Gorden, J. D.; Jones, J. N.; Jones, R. A.; MacDonald, C. L. B. *Chem. Commun*. **2003**, 424. (c) Yu, Z. K.; Heeg, M. J.; Winter, C. H. *Chem. Commun.* **2001**, 353. (d) Korolev, A. V.; Ihara, E.; Guzei, I. A.; Young, V. G., Jr.; Jordan, R. F. *J. Am. Chem. Soc.* **2001**, *123*, 8291. (e) Wochele, R.; Klinkhammer, K. W.; Weidlein, J. *Z. Anorg. Allg. Chem.* **2001**, *627*, 1420. (f) Kickham, J. E.; Guérin, F.; Stewart, J. C.; Urbanska, E.; Stephan, D. W. *Organometallics* **2001**, *20*, 1175. (g) Yu, Z. K.; Wittbrodt, J. M.; Heeg, M. J.; Schlegel, H. B.; Winter, C. H. *J. Am. Chem. Soc*. **2000**, *122*, 9338. (h) McGrady, G. S.; Turner, J. F. C.; Ibberson, R. M.; Prager, M. *Organometallics* **2000**, *19*, 4398. (i) Chen, E. Y.-X.; Abboud, K. A. *Organometallics* **2000**, *19*, 5541. (j) Kickham, J. E.; Guérin, F.; Stewart, J. C.; Stephan, D. W. *Angew. Chem., Int. Ed.* **2000**, *39*, 3263. (k) Wochele, R.; Schwarz, W.; Klinkhammer, K. W.; Locke, K.; Weidlein, J. *Z. Anorg. Allg. Chem.* **2000**, *626*, 1963. (l) Cottone, A., III; Scott, M. J. *Organometallics* **2000**, *19*, 5254. (m) Klosin, J.; Roof, G. R.; Chen, E. Y.-X.; Abboud, K. A. *Organometallics* **2000**, *19*, 4684. (n) Waezsada, S. D.; Rennekamp, C.; Roesky, H. W.; Röpken, C.; Parsini, E. *Z. Anorg. Allg. Chem.* **1998**, *624*, 987. (o) Ihara, E.; Young, V. G., Jr.; Jordan, R. F. *J. Am. Chem. Soc.* **1998**, *120*, 8277. (p) Waezsada, S. D.; Liu, F.-Q.; Murphy, E. F.; Roesky, H. W.; Teichert, M.; Usón, I.; Schmidt, H.-G.; Albers, T.; Parsini, E.; Noltemeyer, M. *Organometallics* **1997**, *16*, 1260.

(3) (a) Malone, J. F.; McDonald, W. S. *Chem. Commun.* **1967**, 444. (b) Malone, J. F.; McDonald, W. S. *J. Chem. Soc., Dalton Trans*. **1972**, 2646. (c) Malone, J. F.; McDonald, W. S. *J. Chem. Soc., Dalton Trans*. **1972**, 2649. (d) Brauer, D. J.; Kruger, C. *Z. Naturforsch.* **1979**, *34B*, 1293. (e) Barber, M.; Liptak, D.; Oliver, J. P. *Organometallics* **1982**, *1*, 1307.

(4) (a) Uhl, W.; Breher, F.; Mbonimana, A.; Gauss, J.; Haase, D.; Lützen, A.; Saak, W. *Eur. J. Inorg. Chem.* **2001**, 3059. (b) Uhl, W.; Breher, F.; Lützen, A.; Saak, W. *Angew. Chem., Int. Ed.* **2000**, *39*, 406. (c) Uhl, W.; Breher, F.; Grunenberg, J.; Lützen, A.; Saak, W. *Organometallics* **2000**, *19*, 4536. (d) Korolev, A. V.; Guzei, I. A.; Jordan, R. F. *J. Am. Chem. Soc.* **1999**, *121*, 11605. (e) Erker, G.; Albrecht, M.; Krüger, C.; Nolte, M.; Werner, S. *Organometallics* **1993**, *12*, 4979. (f) Albright, M. J.; Butler, W. M.; Anderson, T. J.; Glick, M. D.; Oliver, J. P. *J. Am. Chem. Soc.* **1976**, *98*, 3995. (g) Stucky, G. D.; McPherson, A. M.; Rhine, W. E.; Eisch, J. J.; Considine, J. L. *J. Am. Chem. Soc*. **1974**, *96*, 1941.

(5) (a) Tecle, B.; Ilsley, W. H.; Oliver, J. P. *Inorg. Chem.* **1981**, *20*, 2335. (b) Cowley, A. H.; Brown, D. S.; Decken, A.; Kamepalli, S. *Chem. Commun.* **1996**, 2425.

(6) Rahbarnoohi, H.; Kumar, R.; Heeg, M. J.; Oliver, J. P. *Organometallics* **1994**, *13*, 3300.

(7) (a) Althoff, A.; Jutzi, P.; Lenze, N.; Neumann, B.; Stammler, A.; Stammler, H.-G. *Organometallics* **2002**, *21*, 3018. (b) Scholz, S.; Green, J. C.; Lerner, H.-W.; Bolte, M.; Wagner, M. *Chem. Commun.* **2002**, 36. (c) Jutzi, P.; Lenze, N.; Neumann, B.; Stammler, H.-G. *Angew. Chem., Int. Ed.* **2001**, *40*, 1424. (d) Uhl, W.; Hahn, I.; Jantschak, A.; Spies, T. *J. Organomet. Chem.* **2001**, *637*, 300. (e) Hecht, E. *Z. Anorg. Allg. Chem.* **2000**, *626*, 759. (f) Beachey, O. T., Jr.; Rosenblum, D. B.; Churchill, M. R.; Lake, C. H.; Krajkowski, L. M. *Organometallics* **1995**, *14*, 4402. (g) Lee, B.; Pennington, W. T.; Laske, J. A.; Robinson, G. H. *Organometallics* **1990**, *9*, 2864.

(8) For selected leading references, see: (a) Jones, J. N.; Macdonald, C. L. B.; Gorden, J. D.; Cowley, A. H. *J. Organomet. Chem.* **2003**, *666*, 3. (b) Cowley, A. H.; Macdonald, C. L. B.; Silverman, J. S.; Gorden, J. D.; Voigt, A. *Chem. Commun.* **2001**, 175. (c) Dashti-Mommertz, A.; Neumuller, B.; Melle, S.; Haase, D.; Uhl, W. *Z. Anorg. Allg. Chem.* **1999**, *625*, 1828. (d) Beachley, O. T., Jr.; Robirds, E. S.; Atwood, D. A.; Wei, P. *Organometallics* **1999**, *18*, 2561. (e) Schumann, H.; Kucht, H.; Kucht, A.; Görlitz, F. H.; Dietrich, A. *Z. Naturforsch.* **1992**, *47B*, 1241. (f) Beachley, O. T., Jr.; Lees, J. F.; Rogers, R. D. *J. Organomet. Chem.* **1991**, *418*, 165. (g) Beachley, O. T., Jr.; Pazik, J. C.; Glassman, T. E.; Churchill, M. R.; Fettinger, J. C.; Blom, R. *Organometallics* **1988**, *7*, 1051.

(9) Schulte, M.; Gabbaï, F. P. *Chem. Eur. J.* **2002**, *8*, 3802.

(10) Englert, U.; Herberich, G. E.; Rosenplänter, J. *Z. Anorg. Allg. Chem.* **1997**, *623*, 1098.

(11) Malone, J. F.; McDonald, W. S. *J. Chem. Soc.* **1970**, 3362.

(12) (a) Mitzel, N. W.; Lustig, C.; Berger, R. J. F.; Runeberg, N. *Angew. Chem., Int. Ed.* **2002**, *41*, 2519. (b) Boese, R.; Downs, A. J.; Greene, T. M.; Hall, A. W.; Morrison, C. A.; Parsons, S. *Organometallics* **2003**, *22*, 2450. (c) Blake, A. J.; Cradock, S. *J. Chem. Soc., Dalton Trans.* **1990**, 2393. (d) Amma, E. L.; Rundle, R. E. *J. Am. Chem. Soc.* **1958**, *80*, 4141.

(13) Sirimanne, C. T.; Knox, J. E.; Heeg, M. J.; Schlegel, H. B.; Winter, C. H. *J. Am. Chem. Soc.* **2003**, *125*, 11152.

Synthesis of Dimeric Pyrazolate-Bridged Gallium and Indium Complexes Containing Terminal Phenyl Groups. Treatment of triphenylgallium (1 equiv) with 3,5-di-*tert*-butylpyrazole (1 equiv) afforded bis(μ-3,5-di-*tert*-butylpyrazolato)tetraphenyldigallium (**5**, 63%) as an off-white crystalline solid (eq 2). Similarly, treatment of triphenylindium (1−2 equiv) with 3,5-diphenylpyrazole or 3,5-dimethylpyrazole afforded bis(μ-3,5-diphenylpyrazolato)tetraphenyldiindium (**6**, 40%) and bis(μ-3,5-dimethylpyrazolato)tetraphenyldiindium (**7**, 92%), respectively, as colorless crystalline solids. The structural assignments for **5**−**7** were based on spectral and analytical data and X-ray crystal structure determinations. Treatment of 3,5-dimethylpyrazole or 3,5-diphenylpyrazole with large excesses of triphenylindium as a possible route to analogues of **4**·$(C_6H_{14})_{0.5}$ gave several products that appeared from ^{1}H NMR analyses to correspond to mixtures of **6** or **7**, the analogues of **4**·$(C_6H_{14})_{0.5}$, and the unreacted triphenylindium. It was not possible to isolate the analogues of **4**·$(C_6H_{14})_{0.5}$ as pure samples by fractional crystallization, so these reactions were not pursued further.

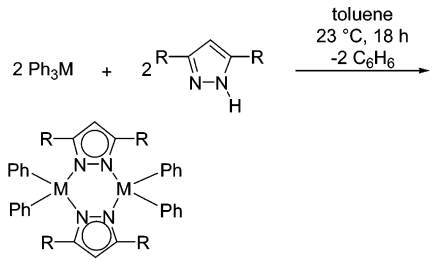

(2)

Attempts to Prepare a Bridging Methyl Complex of Gallium. Encouraged by the stability of **1**, **2**·C_7H_8, **3**, and **4**·$(C_6H_{14})_{0.5}$, we explored the synthesis of the bridging methyl analogue. Treatment of 3,5-di-*tert*-butylpyrazole with trimethylgallium (2 equiv) in hexane at ambient temperature, followed by fractional crystallization from hexane, afforded bis(μ-3,5-di-*tert*-butylpyrazolato)tetramethyldigallium (**8**, 82%) as a colorless crystalline solid (eq 3). The structure of **8** was established from spectral and analytical data. While **8** was not structurally characterized, due to the inability to grow single crystals of sufficient quality, several similar dimeric gallium and indium pyrazolato complexes have been reported.[14] Inspection of the ^{1}H NMR spectrum of crude **8** indicated a 95:5 mixture of **8** and a new complex **9** with resonances that could possibly correspond to the bridging methyl complex $Me_2Ga(\mu$-$tBu_2pz)(\mu$-Me)$GaMe_2$. In particular, the ^{1}H NMR spectrum of **9** revealed resonances with a ratio of 4:1 at δ 0.07 for the gallium-bound methyl groups and at δ 3.25 for another methyl group. In $Me_2Al(\mu$-$R_2pz)(\mu$-Me)$AlMe_2$ (R = Me, Ph, tBu),[2g] the bridging methyl groups exhibited a downfield chemical shift of δ 0.3−0.4 compared to the terminal methyl groups, which is quite different than the downfield shift of δ 3.18 observed in **9**. It was found that pure **9** could be isolated in 2.6% yield by sublimation at 60 °C/0.01 Torr of the residue left after fractional crystallization of **8**. An X-ray crystal structure established that **9** corresponds to the bridging methoxo complex and not the bridging methyl complex. The methoxo ligand in **9** probably originates through insertion of dioxygen into a gallium−methyl bond. Such an oxidation could either occur in trimethylgallium prior to formation of **9** or could occur in a putative bridging methyl complex. If great care was not taken to exclude air from the reaction vessels, much higher yields of **9** were obtained. Variable-temperature ^{1}H NMR spectra between −80 and 20 °C of a mixture of trimethylgallium (5 equiv) and 3,5-di-*tert*-butylpyrazole (1 equiv) in toluene-d_8 showed no evidence for new complexes other than **8** and **9**. Thus, there was no evidence for the formation of a bridging methyl complex similar to the bridging phenyl complexes **1**, **2**·C_7H_8, **3**, and **4**·$(C_6H_{14})_{0.5}$.

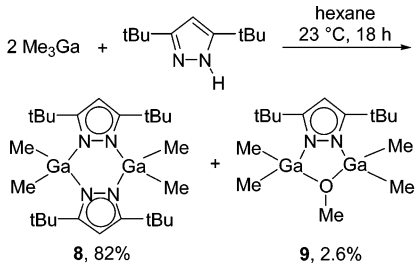

(3)

X-ray Structural Characterization. To establish the solid-state geometries, the X-ray crystal structures of **1**, **2**·C_7H_8, **3**·$(C_6H_{14})_{0.5}$, **4**·$(C_6H_{14})_{0.5}$, **5**−**7**, and **9** were determined. The crystal structure of **1** was described in our preliminary communication.[13] In this section, the structures of **2**·C_7H_8, **3**·$(C_6H_{14})_{0.5}$, **4**·$(C_6H_{14})_{0.5}$, **6**, and **9** are discussed. The molecular structures of **5** and **7** are similar to those of **6**, and structural data for these complexes are contained in the Supporting Information. Experimental crystallographic data are summarized in Table 1, selected bond lengths and angles are given in Tables 2−6, and perspective views are presented in Figures 1−5.

The molecular structure of **2**·C_7H_8 is shown in Figure 1. Consistent with the NMR analysis, the molecule consists of a diphenylpyrazolato ligand with a diphenylgallio group bonded to each nitrogen atom. A phenyl group acts as a bridge between the gallium atoms. The geometry about the gallium centers is distorted tetrahedral. The two gallium atoms and the two nitrogen atoms occupy an approximate plane, while the *ipso*-carbon atom of the bridging phenyl group is situated 0.963(4) Å above this plane. The bridging phenyl group is slightly canted toward Ga(2), giving a distinct triphenylgallium unit containing Ga(1). The gallium−nitrogen bond lengths are 2.021(4) and 1.983(4) Å. The gallium−carbon bond lengths lie in the range 1.958(4)−1.972(4) Å for the terminal phenyl groups and are 2.051(5) (to Ga(1)) and 2.254(5) Å (to Ga(2)) for the bridging phenyl group. The gallium−carbon−gallium angle is 95.82(18)°.

Complex **3**·$(C_6H_{14})_{0.5}$ crystallized as a hexane solvate, and its molecular structure is shown in Figure 2. The overall molecular structure is similar to that of **2**·C_7H_8. The synthesis of bulk **3** afforded hexane-free material, and drying experiments revealed that the hexane solvate is lost upon standing at ambient temperature for

(14) (a) Rendle, A. F.; Storr, A.; Trotter, J. *Can. J. Chem.* **1975**, *53*, 2930. (b) Rendle, A. F.; Storr, A.; Trotter, J. *Can. J. Chem.* **1975**, *53*, 2944. (c) Hausen, H.-D.; Locke, K.; Weidlein, J. *J. Organomet. Chem.* **1992**, *429*, C27.

Table 1. Experimental Crystallographic Data for $2\cdot C_7H_8$, $3\cdot(C_6H_{14})_{0.5}$, $4\cdot(C_6H_{14})_{0.5}$, 6, and 9

	$2\cdot C_7H_8$	$3\cdot(C_6H_{14})_{0.5}$	$4\cdot(C_6H_{14})_{0.5}$	**6**	**9**
empirical formula	$C_{52}H_{44}Ga_2N_2$	$C_{44}H_{51}Ga_2N_2$	$C_{44}H_{51}In_2N_2$	$C_{54}H_{42}In_2N_4$	$C_{16}H_{34}Ga_2N_2O$
fw	836.33	747.31	837.51	976.56	409.89
space group	$P\bar{1}$	$P\bar{1}$	$P\bar{1}$	$P2(1)/c$	$P2(1)/c$
a (Å)	10.384(7)	10.4027(9)	10.210(3)	10.226(3)	12.4949(19)
b (Å)	12.324(9)	11.5593(12)	11.723(3)	12.212(4)	9.1385(12)
c (Å)	18.056(14)	18.4424(19)	18.786(6)	18.225(6)	18.617(3)
α (deg)	74.324(16)	89.757(2)	89.051(5)		
β (deg)	85.822(19)	87.640(2)	86.619(7)	101.009(9)	108.656(2)
γ (deg)	71.84(2)	64.239(2)	66.667(7)		
V (Å^3)	2114(3)	1995.3(3)	2061.0(10)	2234.0(13)	2014.1(5)
Z	2	2	2	2	4
T (K)	295(2)	295(2)	295(2)	295(2)	213(2)
λ (Å)	0.71073	0.71073	0.71073	0.71073	0.71073
density calcd (g cm^{-3})	1.314	1.244	1.350	1.452	1.352
μ (mm^{-1})	1.312	1.381	1.149	1.073	2.676
$R(F)^a$ (%)	4.88	3.88	5.25	3.38	3.12
$R_w(F)^b$ (%)	10.02	8.42	10.97	6.48	8.14

^{a} $R(F) = \sum||F_o| - |F_c||/\sum|F_o|$. ^{b} $R_w(F)^2 = [\sum w(F_o^2 - F_c^2)^2/\sum w(F_o^2)^2]^{1/2}$.

Table 2. Selected Bond Lengths (Å) and Angles (deg) for $2\cdot C_7H_8$

Ga(1)−N(1)	2.021(4)
Ga(2)−N(2)	1.983(4)
Ga(1)−C(16)	2.051(5)
Ga(1)−C(22)	1.972(4)
Ga(1)−C(28)	1.967(5)
Ga(2)−C(16)	2.254(5)
Ga(2)−C(34)	1.971(5)
Ga(2)−C(40)	1.958(4)
N(1)−N(2)	1.377(4)
N(1)−Ga(1)−C(16)	97.42(17)
N(1)−Ga(1)−C(22)	109.39(18)
N(1)−Ga(1)−C(28)	108.42(17)
C(16)−Ga(1)−C(22)	113.69(18)
C(16)−Ga(1)−C(28)	110.21(19)
C(22)−Ga(1)−C(28)	115.99(19)
N(2)−Ga(2)−C(16)	94.74(16)
N(2)−Ga(2)−C(34)	111.09(19)
N(2)−Ga(2)−C(40)	111.59(17)
C(16)−Ga(2)−C(34)	110.82(18)
C(16)−Ga(2)−C(40)	107.39(18)
C(34)−Ga(2)−C(40)	118.6(2)
Ga(1)−C(16)−Ga(2)	95.82(18)

Table 3. Selected Bond Lengths (Å) and Angles (deg) for $3\cdot(C_6H_{14})_{0.5}$

Ga(1)−N(1)	2.013(2)
Ga(2)−N(2)	2.004(2)
Ga(1)−C(12)	2.184(2)
Ga(1)−C(18)	1.971(3)
Ga(1)−C(24)	1.969(3)
Ga(2)−C(12)	2.167(3)
Ga(2)−C(30)	1.978(3)
Ga(2)−C(36)	1.970(3)
N(1)−N(2)	1.393(3)
N(1)−Ga(1)−C(12)	98.78(9)
N(1)−Ga(1)−C(18)	103.14(10)
N(1)−Ga(1)−C(24)	122.37(11)
C(12)−Ga(1)−C(18)	110.65(11)
C(12)−Ga(1)−C(24)	105.08(11)
C(18)−Ga(1)−C(24)	115.44(12)
N(2)−Ga(2)−C(12)	103.52(9)
N(2)−Ga(2)−C(30)	105.05(10)
N(2)−Ga(2)−C(36)	113.08(10)
C(12)−Ga(2)−C(30)	102.87(11)
C(12)−Ga(2)−C(36)	109.24(11)
C(30)−Ga(2)−C(36)	121.28(11)
Ga(1)−C(12)−Ga(2)	92.37(10)

>24 h. The two gallium atoms and the *ipso*-carbon atom of the bridging phenyl group define a plane, while the two nitrogen atoms lie 1.070(4) and 0.465(4) Å above this plane. The gallium−nitrogen bond lengths are 2.013(2) and 2.004(2) Å. The gallium−carbon bond lengths lie in the range 1.969(3)−1.978(3) Å for the terminal phenyl groups and are 2.184(2) and 2.167(3) Å for the bridging phenyl group. The gallium−carbon−gallium angle for $3\cdot(C_6H_{14})_{0.5}$ is 92.37(10)°.

Table 4. Selected Bond Lengths (Å) and Angles (deg) for $4\cdot(C_6H_{14})_{0.5}$

In(1)−N(1)	2.238(5)
In(2)−N(2)	2.219(5)
In(1)−C(12)	2.298(7)
In(1)−C(18)	2.145(7)
In(1)−C(24)	2.156(7)
In(2)−C(12)	2.331(6)
In(2)−C(30)	2.152(7)
In(2)−C(36)	2.164(7)
N(1)−N(2)	1.382(7)
N(1)−In(1)−C(12)	100.9(2)
N(1)−In(1)−C(18)	110.1(2)
N(1)−In(1)−C(24)	101.6(2)
C(12)−In(1)−C(18)	110.7(3)
C(12)−In(1)−C(24)	101.5(3)
C(18)−In(1)−C(24)	128.5(3)
N(2)−In(2)−C(12)	96.2(2)
N(2)−In(2)−C(30)	101.8(2)
N(2)−In(2)−C(36)	124.2(3)
C(12)−In(2)−C(30)	110.6(3)
C(12)−In(2)−C(36)	105.5(3)
C(30)−In(2)−C(36)	116.6(3)
In(1)−C(12)−In(2)	94.6(3)

Table 5. Selected Bond Lengths (Å) and Angles (deg) for 6^a

In−N(1)	2.217(3)
In−N(2)′	2.233(3)
In−C(16)	2.137(3)
In−C(22)	2.138(4)
N(1)−N(2)	1.371(4)
N(1)−In−N(2)′	103.48(10)
N(1)−In−C(16)	101.96(14)
N(1)−In−C(22)	104.52(12)
N(2)′−In−C(16)	104.86(13)
N(2)′−In−C(22)	101.22(12)
C(16)−In−C(22)	136.94(16)

^{a} Primed atoms are transformed by $1-x$, $2-y$, and $1-z$.

The molecular structure of $4\cdot(C_6H_{14})_{0.5}$ is shown in Figure 3. The molecular structure is very similar to that of $3\cdot(C_6H_{14})_{0.5}$. The two indium atoms and the *ipso*-carbon atom of the bridging phenyl group define a plane, while the two nitrogen atoms lie 0.573(10) and 1.200(9) Å above this plane. The bridging phenyl group is slightly canted toward In(2), suggesting a distinct triphenylindium unit containing In(1). The indium−nitrogen bond

Table 6. Selected Bond Lengths (Å) and Angles (deg) for 9

Ga(1)−O	1.933(2)
Ga(2)−O	1.934(2)
Ga(1)−N(1)	2.011(2)
Ga(2)−N(2)	2.011(2)
Ga(1)−C(12)	1.964(3)
Ga(1)−C(13)	1.964(2)
Ga(2)−C(15)	1.962(3)
Ga(2)−C(16)	1.963(3)
O−C(14)	1.429(3)
N(1)−N(2)	1.394(2)
Ga(1)−N(1)−N(2)	118.72(12)
Ga(2)−N(2)−N(1)	118.40(12)
O−Ga(1)−N(1)	90.27(6)
O−Ga(2)−N(2)	90.50(6)
Ga(1)−O−C(14)	117.81(16)
Ga(2)−O−C(14)	116.80(16)
Ga(1)−O−Ga(2)	118.11(8)
C(12)−Ga(1)−C(13)	124.44(12)
C(15)−Ga(2)−C(16)	123.36(13)

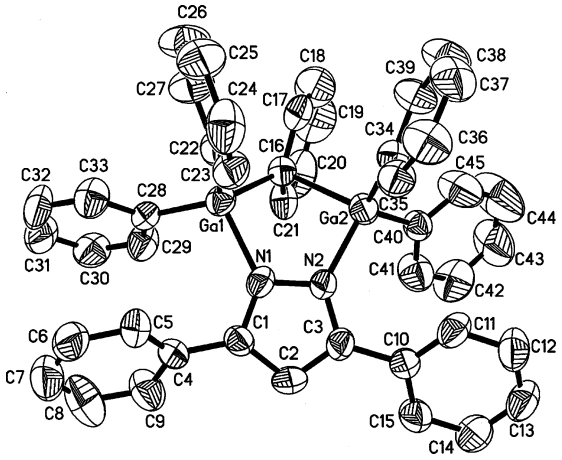

Figure 1. Perspective view of **2**·C_7H_8 with thermal ellipsoids at the 50% probability level.

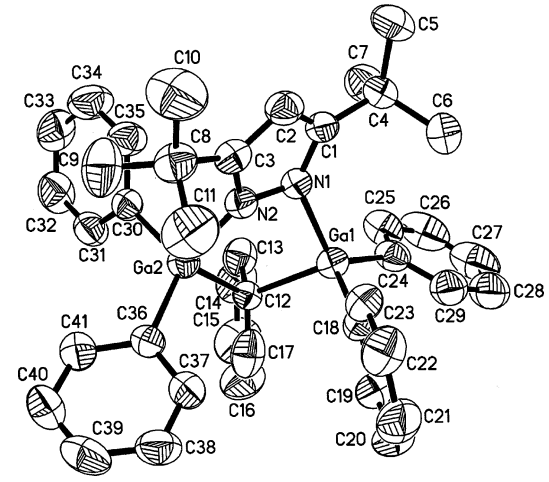

Figure 2. Perspective view of **3**·$(C_6H_{14})_{0.5}$ with thermal ellipsoids at the 50% probability level.

lengths are 2.219(5) and 2.238(5) Å. The indium−carbon bond lengths lie between 2.145(7) and 2.164(7) Å for the terminal phenyl groups and are 2.298(7) and 2.331(6) Å for the bridging phenyl group.

The molecular structure of **6** is shown in Figure 4. It is dimeric with a six-membered In_2N_4 ring and four terminal phenyl groups. Two diphenylpyrazolato ligands serve as bridges between the two indium atoms, and the six-membered In_2N_4 ring consists of four nitrogen

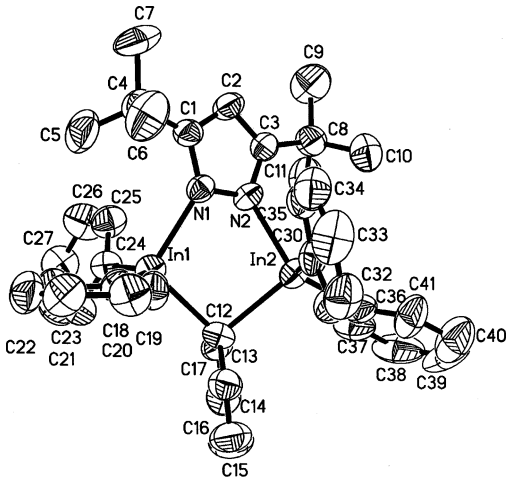

Figure 3. Perspective view of **4**·$(C_6H_{14})_{0.5}$ with thermal ellipsoids at the 50% probability level.

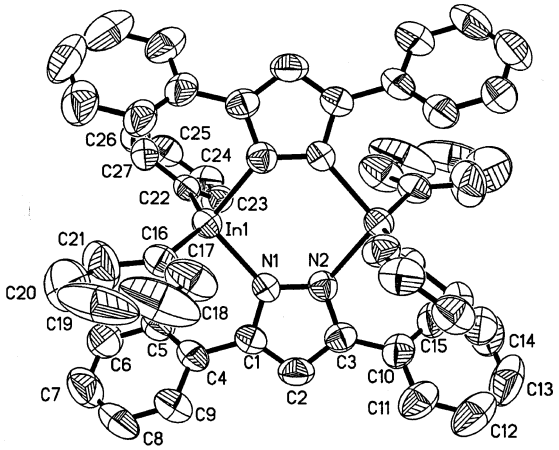

Figure 4. Perspective view of **6** with thermal ellipsoids at the 50% probability level.

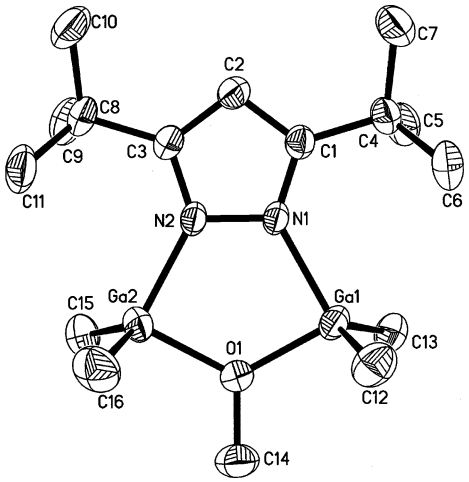

Figure 5. Perspective view of **9** with thermal ellipsoids at the 50% probability level.

atoms from two diphenylpyrazolato ligands and two indium atoms. The geometry about the indium centers is distorted tetrahedral. The indium−nitrogen bond lengths are 2.217(3) and 2.233(3) Å, the indium−carbon bond lengths are 2.137(3) and 2.138(4) Å, and the nitrogen−indium−nitrogen angle is 103.48(10)°.

The molecular structure of **9** is shown in Figure 5. The molecule consists of a 3,5-di-*tert*-butylpyrazolato

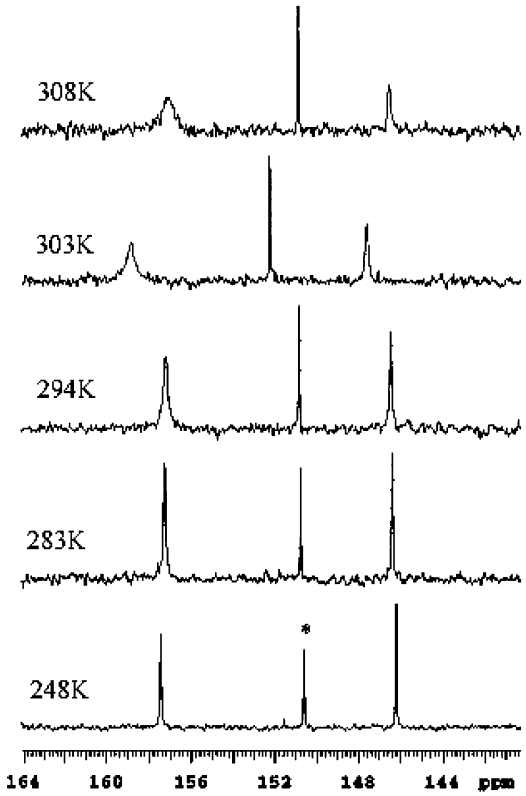

Figure 6. Variable-temperature $^{13}C\{^1H\}$ NMR spectra of **1**. The resonance denoted with an asterisk corresponds to a pyrazolate ring carbon atom.

ligand with a dimethylgallio group bonded to each nitrogen atom. A methoxo ligand acts as a bridge between the two gallium atoms. The gallium and nitrogen atoms occupy an approximate plane, while the methoxo ligand oxygen atom lies 0.383(2) Å above this plane. The gallium−oxygen bond lengths are 1.933(2) and 1.934(2) Å. The gallium−nitrogen bond lengths are both 2.011(2) Å. The gallium−carbon bond lengths are between 1.962(2) and 1.964(3) Å. The gallium−oxygen−gallium angle is 118.11(8)°.

Variable-Temperature NMR Behavior of 1, 2·C_7H_8, 3, and 4·$(C_6H_{14})_{0.5}$. The bridge-terminal phenyl site exchange processes that occur in **1**, **2**·C_7H_8, **3**, and **4**·$(C_6H_{14})_{0.5}$ were studied using NMR spectroscopy. In the $^{13}C\{^1H\}$ NMR spectra in toluene-d_8, the terminal and bridging phenyl groups in **1**, **2**·C_7H_8, **3**, and **4**·$(C_6H_{14})_{0.5}$ (0.106 M) undergo site exchange between −30 and 30 °C. To gain further insight into the dynamic process, the line-broadening kinetics was studied. Figure 6 shows a selected region of the $^{13}C\{^1H\}$ NMR spectrum for **1** taken at various temperatures, showing the *ipso*-carbon atoms of the phenyl ligands. These resonances broaden with increasing temperature and eventually coalesce, which is consistent with bridge-terminal phenyl exchange. Complexes **2**·C_7H_8, **3**, and **4**·$(C_6H_{14})_{0.5}$ show similar $^{13}C\{^1H\}$ NMR spectra and undergo similar phenyl site exchange processes. The phenyl site exchange processes were modeled as AB_4 systems. Rate constants were determined by simulating $^{13}C\{^1H\}$ NMR spectra at various temperatures using the program gNMR.[15] Full kinetics data for **1**, **2**·C_7H_8, **3**, and **4**·$(C_6H_{14})_{0.5}$ are contained in the Supporting Information. Eyring analyses of the rate data for **1**, **2**·C_7H_8, **3**, and **4**·$(C_6H_{14})_{0.5}$ afforded the activation parameters given in Table 7. The enthalpies of activation ($\Delta H^{\ddagger}$) range between 6 and 8.9 kcal/mol, while the entropies of activation ($\Delta S^{\ddagger}$) range between −23.1 and −32.0 eu. The free energies at 298 K for phenyl exchange range between 15.2 and 15.8 kcal/mol. The calculated rate constants at 298 K for phenyl site exchange in **1**, **2**·C_7H_8, **3**, and **4**·$(C_6H_{14})_{0.5}$ range between 15.8 and 40.7 s^{-1}. Analysis of ∼0.05 M solutions of **1**, **2**·C_7H_8, **3**, and **4**·$(C_6H_{14})_{0.5}$ in toluene-d_8 afforded NMR spectra that were identical to those obtained in ∼0.10 M solutions, suggesting that the exchange processes are intramolecular.

(15) *gNMR*; Version 4; Cherwell Scientific Publishing, 1997.

Table 7. Activation Parameters from Eyring Analyses and Rate Constants at 298 K for 1, 2·C_7H_8, 3, and 4·$(C_6H_{14})_{0.5}$

complex	$\Delta H^{\ddagger}$ (kcal/mol)	$\Delta S^{\ddagger}$ (eu)	$\Delta G^{\ddagger}$(298 K) (kcal/mol)	k(298 K) (s^{-1})
1	7.6 ± 0.4	−27.2 ± 1.4	15.7 ± 1.8	20.1
2·C_7H_8	6.0 ± 0.3	−32.0 ± 1.2	15.5 ± 1.5	24.8
3	8.9 ± 0.5	−23.1 ± 1.8	15.8 ± 2.3	15.8
4·$(C_6H_{14})_{0.5}$	6.1 ± 0.4	−30.5 ± 1.4	15.2 ± 1.8	40.7

Discussion

The molecular structures of **1**, **2**·C_7H_8, **3**·$(C_6H_{14})_{0.5}$, and **4**·$(C_6H_{14})_{0.5}$ provide an opportunity to examine the characteristics associated with bridging phenyl ligands in gallium and indium complexes. In the series **1**, **2**·C_7H_8, and **3**·$(C_6H_{14})_{0.5}$, the gallium−carbon bond lengths associated with the terminal phenyl ligands fall within a narrow range of 1.958−1.978 Å. These values are very similar to those found in $GaPh_3$ (1.946(7), 1.968(5) Å)[11] and are consistent with normal gallium−phenyl bonds. The gallium−nitrogen bond distances are roughly similar across the series **1**, **2**·C_7H_8, and **3**·$(C_6H_{14})_{0.5}$ and span 1.967−2.021 Å. The gallium−carbon bond lengths for the bridging phenyl ligand, however, do not follow a clear trend in **1**, **2**·C_7H_8, and **3**·$(C_6H_{14})_{0.5}$. In **1** and **2**·C_7H_8, these bond lengths are asymmetric, with values of 2.114(2) and 2.219(2) Å and 2.051(5) and 2.254(5) Å, respectively. By contrast, the related bond distances in **3**·$(C_6H_{14})_{0.5}$ (2.167(3), 2.184(2) Å) are identical within experimental error. The differences in bridging phenyl gallium−carbon bond lengths in **1**, **2**·C_7H_8, and **3**·$(C_6H_{14})_{0.5}$ could have several origins. The bond strengths associated with the bridging phenyl ligands are probably small, which would allow low-energy distortions in the bond distances during crystallization to achieve optimum crystal packing. The pyrazolato ligand carbon atom substituents in **1**, **2**·C_7H_8, and **3**·$(C_6H_{14})_{0.5}$ also have significantly different steric profiles, which affect the bonding to the pyrazolato ligands. In **1**, the nitrogen and carbon atoms within the Ga_2N_2C ring are approximately coplanar, while one gallium atom is slightly above and the other is slightly below this plane. Since the methyl substituents in **1** have the smallest steric profile, this molecular structure is probably the least distorted of the series. In **2**·C_7H_8, the gallium and nitrogen atoms are approximately coplanar within the Ga_2N_2C ring, and the bridging phenyl *ipso*-carbon atom lies slightly out of this plane. Such an arrangement appears to place the pyrazolato phenyl groups in the sterically least demanding positions. In **3**·$(C_6H_{14})_{0.5}$, severe steric crowding between the pyrazolato *tert*-butyl

substituents and the terminal phenyl ligands leads to considerable twisting of the pyrazolato ligand with respect to an approximate Ga_2C plane. Such twisting of the pyrazolato ligand may force the gallium atoms to form similar bond distances to the bridging phenyl ligand. In **1** and **2**·C_7H_8, the pyrazolato ligands are not as sterically demanding as in **3**·$(C_6H_{14})_{0.5}$, and asymmetric gallium−carbon distances are observed to the bridging phenyl ligand. The molecular structures of **3**·$(C_6H_{14})_{0.5}$ and **4**·$(C_6H_{14})_{0.5}$ are very similar due to their identical ligand framework.

There are few structurally characterized gallium and indium complexes that contain bridging phenyl or similar unsaturated ligands. Gabbaï has reported 1,8-disubstituted naphthalene complexes that contain one dimesitylboron group and either a dichlorogallio or dichloroindio substituent.[9] The *ipso*-carbon atom of one of the boron-bound mesityl groups forms a bridge to the heavier group 13 metal. In the gallium complex, the bridging phenyl gallium−carbon distance is 2.279(4) Å, which is much longer than all but one of the related bond distances in **1**, **2**·C_7H_8, and **3**·$(C_6H_{14})_{0.5}$. In the indium complex, the bridging phenyl indium−carbon distance is 2.442(6) Å, which is longer than the related distances of 2.297(7) and 2.331(6) Å in **4**·$(C_6H_{14})_{0.5}$. In **1**, **2**·C_7H_8, **3**·$(C_6H_{14})_{0.5}$, and **4**·$(C_6H_{14})_{0.5}$, the contiguous nitrogen atoms in the pyrazolato ligands hold the MPh_2 and MPh_3 units closer together than the three-carbon bridges in Gabbaï's 1,8-disubstituted naphthalene complexes. Hence, the metal−carbon bond distances are longer in Gabbaï's complexes than in **1**, **2**·C_7H_8, **3**·$(C_6H_{14})_{0.5}$, and **4**·$(C_6H_{14})_{0.5}$. In the solid-state structure of $InPh_3$,[11] there are intermolecular contacts of 3.07−3.40 Å between the indium atoms and *ipso*-, *ortho*-, and *meta*-carbon atoms of adjacent phenyl ligands. In the solid-state structure of triphenylgallium,[11] there are similar contacts of 3.42−3.81 Å between the gallium atoms and the *ortho*-, *meta*-, and *para*-carbon atoms of adjacent phenyl ligands. The closest homodinuclear comparison to **1**, **2**·C_7H_8, **3**, and **4**·$(C_6H_{14})_{0.5}$ is $[Me_2In(\mu\text{-}2\text{-}C_4H_3S)]_2$,[6] in which 2-thienyl ligands serve as bridges between two indium atoms. This complex has terminal indium−carbon bond lengths between 2.139 and 2.143 Å, highly asymmetric bridging indium−carbon bond lengths of 2.194(6) and 2.849(3) Å, and an indium−carbon−indium angle of 89.4° within the four-membered ring. The related angle for **4**·$(C_6H_{14})_{0.5}$ (96.88(9)°) is larger due to geometric constraints imposed by the five-membered In_2N_2C ring. The bonding associated with the bridging 2-thienyl ligand is clearly very different than the bonding of the bridging phenyl ligands in **1**, **2**·C_7H_8, **3**·$(C_6H_{14})_{0.5}$, and **4**·$(C_6H_{14})_{0.5}$.

The activation parameters for **1**, **2**·C_7H_8, **3**, and **4**·$(C_6H_{14})_{0.5}$ allow insight into the transition states that lead to interconversion of the bridging and terminal phenyl ligands. The activation parameters and calculated rate constants at 298 K shown in Table 7 are very similar for all four bridging phenyl complexes and suggest similar exchange mechanisms. The $\Delta H^{\ddagger}$ values range between 6 and 8.9 kcal/mol and represent small differences in energy between the ground states and the transition states for phenyl site exchange. The $\Delta S^{\ddagger}$ values range from −23.1 to −32.0 eu and suggest transition states that are highly ordered relative to the ground states. Since the metal−nitrogen bond energies should be much stronger than the bridging phenyl bond energies, it is very likely that the transition state is obtained by rotation of a $GaPh_3$ unit along a gallium−nitrogen bond vector. Rotation by 120° would place a terminal phenyl ligand into the bridging position and would convert the bridging phenyl group to a terminal phenyl ligand. Such a transition state is outlined in Scheme 1 and is similar to what we proposed earlier for bridge-terminal methyl exchange in $Me_2Al(\mu\text{-}R_2pz)(\mu\text{-}Me)AlMe_2$.[2g] The large negative $\Delta S^{\ddagger}$ values lead to free energies at 298 K for phenyl exchange that range between 15.2 and 15.8 kcal/mol. Finally, the calculated rate constants at 298 K for phenyl site exchange in **1**, **2**·C_7H_8, **3**, and **4**·$(C_6H_{14})_{0.5}$ range between 15.8 and 40.7 s^{-1}. Thus, the pyrazolato carbon atom substituents and the identity of the metal center have small effects on the rates of exchange.

Scheme 1. Proposed Transition State for Phenyl Ligand Exchange

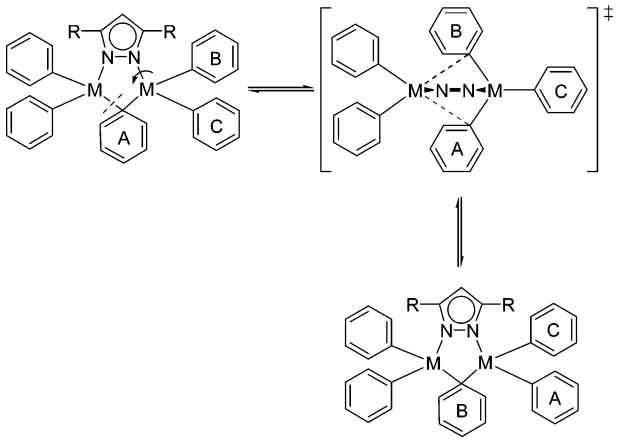

Complexes **5**−**8** form upon treatment of triphenylgallium, triphenylindium, or trimethylgallium with one or more equivalents of 3,5-dimethylpyrazole, 3,5-diphenylpyrazole, or 3,5-di-*tert*-butylpyrazole. The complexes have dimeric structures containing two pyrazolato ligands that bridge between the metal atoms and two terminal phenyl or methyl ligands per metal atom. Several dimeric gallium and indium pyrazolato complexes of the formula $[Me_2M(pz)]_2$ (pz = pyrazolato or substituted pyrazolato ligands) have been structurally characterized and have structures that are very similar to those of **5**−**8**.[14] Complexes **5**−**8** appear to be very stable thermodynamically and once formed are unreactive toward excess MPh_3 or MMe_3. In the case of **6** and **7**, these dimeric complexes are the major products even when two or more equivalents of triphenylindium are employed. The failure to form the analogues of **4**·$(C_6H_{14})_{0.5}$ in high yields upon treatment of triphenylindium with 2 equiv of 3,5-dimethylpyrazole or 3,5-diphenylpyrazole suggests either that **6** and **7** form rapidly and do not convert to the phenyl-bridged complexes in the presence of excess triphenylindium or that the analogues of **4**·$(C_6H_{14})_{0.5}$ are unstable and decompose rapidly to **6** and **7**. We were also unsuccessful in our attempts to prepare a bridging methyl complex of gallium through treatment of 3,5-di-*tert*-butylpyrazole with excess trimethylgallium. The major product was the dimeric complex **8**, and the minor product, **9**, was determined to be a bridging methoxo complex by X-ray

crystallography. It is likely that in a methyl-bridged complex with a structure similar to those of **1**, **2**·C_7H_8, **3**, and **4**·$(C_6H_{14})_{0.5}$, a methyl bridge does not provide enough bond energy to stabilize the complex relative to **8**.

In our report of bridging methyl complexes of the formula $Me_2Al(\mu\text{-}R_2pz)(\mu\text{-}Me)AlMe_2$,[2g] molecular orbital calculations demonstrated that the bridging methyl ligand is stabilized by through-space bonding with pyrazolato-based π-orbitals and that these interactions contribute to the stability of these complexes. In our preliminary communication describing **1**, **2**·C_7H_8, and **3**, we described molecular orbital calculations of the model complex $H_2Ga(\mu\text{-}C_3H_3N_2)(\mu\text{-}C_6H_5)GaH_2$.[13] In the optimized structure, the gallium and nitrogen atoms occupy an approximate plane, with the bridging phenyl carbon atom lying above this Ga_2N_2 plane. The optimized structure of $H_2Ga(\mu\text{-}C_3H_3N_2)(\mu\text{-}C_6H_5)GaH_2$ and the solid-state structure of **2** thus have similar Ga_2N_2C core structures. However, the difference between a planar Ga_2N_2C ring in $H_2Ga(\mu\text{-}C_3H_3N_2)(\mu\text{-}C_6H_5)GaH_2$ and one with a bent carbon atom was calculated to be only 1.77 kcal/mol. Thus, through-space bonding interactions between the bridging phenyl ligand and pyrazolato-based orbitals provide very little stabilization to $H_2Ga(\mu\text{-}C_3H_3N_2)(\mu\text{-}C_6H_5)GaH_2$. Instead, the stability of the bridging phenyl ligand in $H_2Ga(\mu\text{-}C_3H_3N_2)(\mu\text{-}C_6H_5)GaH_2$, **1**, **2**·$C_7H_8$, **3**, and **4**·$(C_6H_{14})_{0.5}$ appears to arise from strong gallium−nitrogen bonds that hold the two metal atoms in close proximity and allow a weak bridging interaction to exist. The results of this work suggest that appropriate ligand design could lead to many new examples of homometallic heavier group 13 complexes that contain bridging hydrocarbon ligands.

We have been so far unsuccessful in our attempts to prepare a bridging methyl complex of gallium. However, the present work was inspired by weak, long (>3.0 Å) metal−carbon contacts in the solid-state structures of gallium and indium phenyl[11] complexes and by the successful synthesis of heterobimetallic group 13 complexes with bridging phenyl ligands.[9] Reports of long metal−carbon contacts in the solid-state structures of the heavier group 13 alkyl complexes[12] suggest that it still may be possible to stabilize a bridging methyl complex of gallium or indium. We continue to work toward this and other goals with group 13 complexes.

Experimental Section

General Considerations. All manipulations were carried out under argon using Schlenk line or glovebox techniques. Hexane and toluene were distilled from sodium immediately prior to use. 3,5-Dimethylpyrazole, benzene-d_6, and toluene-d_8 were purchased from Aldrich Chemical Co. 3,5-Diphenylpyrazole and 3,5-di-*tert*-butylpyrazole were prepared according to a published procedure.[16] Triphenylgallium[17] and triphenylindium[18] were prepared according to published procedures.

^1H and $^{13}C\{^1H\}$ NMR spectra were recorded at 500, 300, 125, or 75 MHz in benzene-d_6 or toluene-d_8, as indicated. Chemical shifts (δ, ppm) are given relative to residual protons or the carbon atoms of the indicated solvent. Infrared spectra were obtained using Nujol as the medium. Microanalyses were performed by Midwest Microlab, Indianapolis, IN. Melting points were determined in sealed capillary tubes under argon on a Haake-Buchler HBI digital melting point apparatus and are uncorrected.

Synthesis of $(C_6H_5)_2Ga(\mu\text{-}\eta^1\text{:}\eta^1\text{-}3,5\text{-}Me_2pz)(\mu\text{-}C_6H_5)Ga(C_6H_5)_2$ (1). To a stirred solution of triphenylgallium (0.602 g, 2.00 mmol) in toluene (40 mL) was added dropwise a solution of 3,5-dimethylpyrazole (0.096 g, 1.00 mmol) in toluene (30 mL). The reaction mixture was stirred at room temperature for 18 h, and the volatile components were removed under reduced pressure to afford a white solid. The resultant solid was extracted with hexane (280 mL), filtered through a 2 cm pad of Celite, and concentrated. Complex **1** was isolated as colorless single crystals at room temperature (0.385 g, 62%): mp 161−162 °C; IR (Nujol, cm^{-1}) 3060 (w), 3037 (w), 2955 (s), 2927 (s), 2851 (s), 1571 (w), 1529 (m), 1425 (m), 1056 (w), 1038 (w), 989 (w), 702 (s), 665 (w); ^1H NMR (benzene-d_6, 23 °C, δ) 8.43 (br m, 2H, bridging Ph-*H*), 7.48, 7.18 (m, 20 H, terminal Ph-*H*), 6.79 (br m, 1H, bridging Ph-*H*), 6.68 (br m, 2H, bridging Ph-*H*), 5.78 (s, 1H, pz ring C*H*), 1.94 (s, 6H, CH_3); $^{13}C\{^1H\}$ NMR (benzene-d_6, 23 °C, ppm) 157.3 (br s, *ipso-C*, bridging phenyl ring), 150.85 (s, pz ring *C*-CH_3), 146.5 (br s, *ipso-C*, terminal phenyl rings), 137.50 (br s, *ortho-C*-H, bridging phenyl ring), 136.53 (s, *ortho-C*-H, terminal phenyl rings), 128.15 (br s, *meta-C*-H, bridging phenyl ring), 128.00 (s, *para-C*-H, bridging phenyl ring), 127.92 (s, *meta-C*-H, terminal phenyl rings), 127.76 (s, *para-C*-H, terminal phenyl rings), 108.05 (s, pz ring *C*H), 13.02 (s, C-*C*H_3). Anal. Calcd for $C_{35}H_{32}Ga_2N_2$: C, 67.79; H, 5.20; N, 4.52. Found: C, 67.69; H, 5.29; N, 4.64.

Synthesis of $(C_6H_5)_2Ga(\mu\text{-}\eta^1\text{:}\eta^1\text{-}3,5\text{-}Ph_2pz)(\mu\text{-}C_6H_5)Ga(C_6H_5)_2\cdot C_7H_8$ (2·C_7H_8). In a fashion similar to the preparation of **1**, treatment of triphenylgallium (0.602 g, 2.00 mmol) with 3,5-diphenylpyrazole (0.220 g, 1.00 mmol) in toluene afforded **2**·C_7H_8 (0.521 g, 62%) as colorless single crystals after crystallization from toluene at −20 °C: mp 186−187 °C; IR (Nujol, cm^{-1}) 3055 (w), 3041 (w), 2945 (s), 2925 (s), 2855 (s), 1572 (w), 1539 (w), 1425 (m), 1104 (m), 761 (m), 698 (s); ^1H NMR (benzene-d_6, 23 °C, δ) 8.41 (br m, 2H, bridging Ph-*H*), 7.61 (m, 10H, pz ring Ph-*H*), 7.35−7.07 (br m, 20H, terminal Ph-*H*), 6.81 (s, 1H, pz ring C*H*), 6.67 (br m, 3H, bridging Ph-*H*); $^{13}C\{^1H\}$ NMR (benzene-d_6, 23 °C, ppm) 157.85 (br s, *ipso-C*, bridging phenyl ring), 156.50 (s, pz ring *C*-Ph), 146.45 (br s, *ipso-C*, terminal phenyl rings), 139.2 (br s, *ortho-C*-H, bridging phenyl ring), 136.54 (br s, *ortho-C*-H, terminal phenyl ring), 125−131 (overlapping resonances from terminal and bridging gallium-phenyl, pyrazolato phenyl groups), 107.24 (s, pz ring *C*-H). Anal. Calcd for $C_{52}H_{44}Ga_2N_2$: C, 74.68; H, 5.30; N, 3.35. Found: C, 74.29; H, 5.19; N, 3.49.

Synthesis of $(C_6H_5)_2Ga(\mu\text{-}\eta^1\text{:}\eta^1\text{-}3,5\text{-}tBu_2pz)(\mu\text{-}C_6H_5)Ga(C_6H_5)_2$ (3). In a fashion similar to the preparation of **1**, treatment of triphenylgallium (0.602 g, 2.00 mmol) with 3,5-di-*tert*-butylpyrazole (0.180 g, 1.00 mmol) in toluene afforded **3** (0.282 g, 40%) as colorless single crystals after crystallization from hexane at −20 °C: mp 149−151 °C; IR (Nujol, cm^{-1}) 3052 (w), 3037 (w), 2955 (s), 2925 (s), 2855 (s), 1571 (w), 1511 (w), 1426 (w), 701 (m); ^1H NMR (benzene-d_6, 23 °C, δ) 8.50 (br m, 2H, bridging Ph-*H*), 7.32−7.15 (m, 20 H, terminal Ph-*H*), 6.79 (br m, 1H, bridging Ph-*H*), 6.69 (br m, 2H, bridging Ph-*H*), 6.39 (s, 1H, pz ring C-*H*), 1.22 (s, 18H, C(CH_3)$_3$); $^{13}C\{^1H\}$ NMR (benzene-d_6, 23 °C, ppm) 165.86 (s, pz ring *C*-C(CH_3)$_3$), 158. 33 (br s, *ipso-C*, bridging phenyl rings), 148.26 (br s, *ipso-C* of terminal phenyl rings), 136.93 (br s, *ortho-C*-H, bridging phenyl ring), 128.42 (br s, *meta-C*-H, bridging phenyl ring), 128.15 (s, *ortho-* or *meta-C*-H, terminal phenyl rings), 128.00 (s, *para-C*-H, bridging phenyl ring), 127.81 (s, *para-C*-H, terminal phenyl rings), 127.68 (s, *ortho-* or *meta-C*-H, terminal phenyl rings), 104.28 (s, pz ring *C*-H), 32.70 (s, *C*(CH_3)$_3$), 31.33

(16) Elguéro, J.; Gonzalez, E.; Jacquier, R. *Bull. Soc. Chim. Fr.* **1968**, 707.
(17) Xiushan, Z.; Xiaolin, Z.; Lei, F.; Wentian, T. *Huaxue Shiji* **1997**, *19*, 246.
(18) Viktorova, I. M.; Endovin, Yu. P.; Sheverdina, N. I.; Kocheshkov, K. A. *Dokl. Akad. Nauk. SSSR* **1967**, *177*, 103.

(s, C(CH_3)$_3$). Anal. Calcd for $C_{41}H_{44}Ga_2N_2$: C, 69.59; H, 6.60; N, 4.02. Found: C, 69.92; H, 6.30; N, 3.98. Even though the X-ray crystallographic determination was consistent with a formulation of **3**·$(C_6H_{14})_{0.5}$, **3** was isolated as the solvent-free material in the bulk synthesis. The hexane solvate is loosely held and is readily lost upon standing at ambient temperature.

Synthesis of $(C_6H_5)_2In(\mu\text{-}\eta^1\text{:}\eta^1\text{-}3,5\text{-}tBu_2pz)(\mu\text{-}C_6H_5)In(C_6H_5)_2\cdot(C_6H_{14})_{0.5}$ (4·$(C_6H_{14})_{0.5}$). In a fashion similar to the preparation of **1**, treatment of triphenylindium (0.692 g, 2.00 mmol) with 3,5-di-*tert*-butylpyrazole (0.180 g, 1.00 mmol) in toluene afforded **4**·$(C_6H_{14})_{0.5}$ (0.335 g, 40%) as colorless crystals after crystallization from hexane at −20 °C: mp 159−160 °C; IR (Nujol, cm^{-1}) 3055 (w), 3033 (w), 1569 (w), 1506 (w), 1421 (w), 701 (m); ^{1}H NMR (toluene-d_8, 4 °C, δ) 8.28 (br m, 2H, bridging Ph-*H*), 7.26−7.14 (br m, 20H, terminal Ph-*H*), 6.87 (br m, 3H, bridging Ph-*H*), 6.33 (s, 1H, pz ring C-*H*), 1.28 (s, 18H, C(CH_3)$_3$); ^{13}C{^{1}H} NMR (toluene-d_8, 4 °C, ppm) 166.16 (s, pz ring *C*-C(CH_3)$_3$), 151.63 (br s, *ipso-C*, bridging, terminal phenyl rings), 138.24 (br s, *ortho-C*-H, bridging, terminal phenyl rings), 127−129 (*meta*- and para-C-H of bridging, bridging phenyl rings obscured by toluene-d_8 resonances), 102.12 (s, pz ring *C*-H), 32.32 (s, *C*(CH_3)$_3$), 31.32 (s, C(*C*H_3)$_3$). Anal. Calcd for $C_{44}H_{51}In_2N_2$: C, 63.10; H, 6.14; N, 3.34. Found: C, 62.89; H, 6.14; N, 3.20.

Synthesis of $(C_6H_5)_2Ga(\mu\text{-}\eta^1\text{:}\eta^1\text{-}3,5\text{-}tBu_2pz)_2Ga(C_6H_5)_2$ (5). To a stirred solution of triphenylgallium (0.325 g, 0.87 mmol) in toluene (40 mL) was added a solution of 3,5-di-*tert*-butylpyrazole (0.156 g, 0.87 mmol) in toluene (30 mL). The reaction mixture was stirred at room temperature for 18 h, and the volatile components were then removed under reduced pressure to afford an off-white solid. This solid was dissolved in hexane (70 mL). The resultant solution was filtered through a 2 cm pad of Celite, and the filtrate was concentrated to a volume of about 30 mL under reduced pressure. Complex **5** formed as colorless crystals at −20 °C and was isolated by removal of the hexane solution using a cannula, followed by vacuum-drying of the crystals (0.253 g, 63%): mp 176−178 °C; IR (Nujol, cm^{-1}) 3064 (w), 3043 (w), 1516 (m), 1428 (w), 1401 (w), 1211 (w), 1086 (m); ^{1}H NMR (benzene-d_6, 23 °C, δ) 7.86 (m, 8H, Ph-*H*), 7.26 (m, 8H, Ph-*H*), 7.17 (m, 4H, Ph-*H*), 6.10 (s, 2H, pz ring C-*H*), 1.17 (s, 36H, C(CH_3)$_3$); ^{13}C{^{1}H} NMR (benzene-d_6, 23 °C, ppm) 170.28 (s, pz ring *C*-C(CH_3)$_3$), 148.74 (s, *ipso-C*, phenyl rings), 137.01 (s, *ortho-C*, phenyl rings), 128.13 (s, *meta-C*, phenyl rings), 127.80 (s, *para-C*, phenyl rings), 108.18 (s, pz ring *C*-H), 32.72 (s, *C*(CH_3)$_3$), 31.26 (s, C(*C*H_3)$_3$). Anal. Calcd for $C_{46}H_{58}Ga_2N_4$: C, 68.51; H, 7.25; N, 6.95. Found: C, 66.72; H, 7.13; N, 7.01.

Synthesis of $(C_6H_5)_2In(\mu\text{-}\eta^1\text{:}\eta^1\text{-}3,5\text{-}Ph_2pz)_2In(C_6H_5)_2$ (6). In a fashion similar to the synthesis of **5**, treatment of triphenylindium (0.346 g, 1.00 mmol) with 3,5-diphenylpyrazole (0.220 g, 1.00 mmol) in toluene afforded **6** (0.205 g, 40%) as colorless rods after crystallization from hexane at −20 °C: mp 220−222 °C; IR (Nujol, cm^{-1}) 3112 (w), 3052 (w), 1537 (w), 1426 (w), 1392 (w), 1273 (w), 918 (w), 698 (s); ^{1}H NMR (benzene-d_6, 23 °C, δ) 7.51 (m, 16 H, pz ring Ph-*H*), 7.31 (m, 8H, terminal Ph-*H*), 7.26 (m, 8H, terminal Ph-*H*), 7.11 (m, 4H, terminal Ph-*H*), 6.85 (m, 4H, pz ring Ph-*H*), 6.46 (s, 2H, pz ring C-*H*); ^{13}C{^{1}H} NMR (benzene-d_6, 23 °C, ppm) 159.21 (s, pz ring *C*-Ph), 150.93 (s, *ipso-C*, terminal phenyl rings), 137.81 (s, *ortho-C*-H of terminal phenyl rings), 132.60 (s, *ipso-C*-H of pz phenyl rings), 129.36 (s, *ortho-C*-H of pz phenyl rings), 128.81 (s, para-*C*-H of pz phenyl rings), 128.60 (s, *meta-C*-H of pz phenyl rings), 127.7−127.3 (meta-*C*-H of terminal phenyl rings obscured by C_6D_6 resonances), 107.08 (s, pz ring *C*H). Anal. Calcd for $C_{54}H_{42}In_2N_4$: C, 66.41; H, 4.33; N, 5.74. Found: C, 66.54; H, 4.50; N, 5.55.

Synthesis of $(C_6H_5)_2In(\mu\text{-}\eta^1\text{:}\eta^1\text{-}3,5\text{-}Me_2pz)_2In(C_6H_5)_2$ (7). In a fashion similar to the synthesis of **5**, treatment of triphenylindium (0.346 g, 1.00 mmol) with 3,5-dimethylpyrazole (0.096 g, 1.00 mmol) in toluene afforded **7** (0.335 g, 92%) as a colorless crystalline solid after crystallization from hexane at −20 °C: mp 228 °C; ^{1}H NMR (benzene-d_6, 23 °C, δ) 7.60 (m, 8H, Ph-*H*), 7.17 (m, 12H, Ph-*H*), 5.63 (s, 2H, pz ring C-*H*), 2.03 (s, 12H, CH_3); ^{13}C{^{1}H} NMR (benzene-d_6, 23 °C, ppm) 152.40 (s, pz ring *C*-CH_3), 149.61 (s, *ipso-C* of phenyl rings), 138.35 (s, *ortho-C*-H of phenyl rings), 128.68 (s, *meta-C*-H of phenyl rings), 128.47 (s, *para-C*-H of terminal phenyl rings), 106.89 (s, pz ring *C*-H), 13.71 (s, C-*C*H_3). Anal. Calcd for $C_{34}H_{34}In_2N_4$: C, 56.07; H, 4.71; N, 7.69. Found: C, 54.17; H, 4.83; N, 7.06.

Synthesis of $Me_2Ga(\mu\text{-}\eta^1\text{:}\eta^1\text{-}3,5\text{-}tBu_2pz)_2GaMe_2$ (8) and $Me_2Ga(\mu\text{-}\eta^1\text{:}\eta^1\text{-}3,5\text{-}tBu_2pz)(\mu\text{-}OMe)GaMe_2$ (9). A solution of 3,5-di-*tert*-butylpyrazole (1.80 g, 10.0 mmol) in hexane (100 mL) was cooled to −78 °C. Using a syringe, a 3.0 M solution of trimethylgallium in hexane (20 mL, 60 mmol) was slowly added to the 3,5-di-*tert*-butylpyrazole mixture. The resulting solution was allowed to warm to ambient temperature and was stirred for another 15 h. The volatile components were then removed under reduced pressure. ^{1}H NMR analysis of this crude product indicated a 95:5 mixture of **8** and **9**. The crude product was dissolved in hexane (10 mL). This product was allowed to stand at ambient temperature for 24 h, during which time colorless crystals formed. Isolation of the crystals was effected by cannulation of the mother liquor, followed by vacuum-drying, to afford colorless crystals of **8** (2.29 g, 82%). The volatile components were removed from the mother liquor under reduced pressure, and the residue was then sublimed at 60 °C/0.01 Torr to afford **9** as colorless crystals (0.11 g, 2.6%).

Spectral and analytical data for **8**: mp 163 °C; IR (KBr, cm^{-1}) 3234 (w), 2967 (s), 2928 (s), 2870 (m), 1509 (s), 1461 (s), 1400 (m), 1361 (s), 1295 (s), 1247 (s), 1214 (s), 1200 (s), 1071 (m), 1033 (m), 1004 (m), 928 (w), 804 (s), 747 (s), 628 (s), 576 (s), 528 (s), 447 (m); ^{1}H NMR (benzene-d_6, 23 °C, δ) 6.17 (s, 2H, pz ring C-*H*), 1.30 (s, 36H, C(CH_3)$_3$), −0.19 (s, 12H, Ga-(CH_3)$_2$); ^{13}C{^{1}H} NMR (benzene-d_6, 23 °C, ppm) 169.54 (s, *C*-C(CH_3)$_3$), 105.59 (s, pz ring *C*H), 32.53 (s, *C*(CH_3)$_3$), 31.14 (s, C(*C*H_3)$_3$), −2.42 (s, Ga(*C*H_3)$_2$). Anal. Calcd for $C_{26}H_{50}Ga_2N_4$: C, 55.95; H, 9.03; N, 10.04. Found: C, 55.78; H, 9.01; N, 10.03.

Spectral and analytical data for **9**: mp 79 °C; ^{1}H NMR (benzene-d_6, 23 °C, δ) 6.10 (s, 1H, pz ring C-*H*), 3.25 (s, 3H, Ga-OCH_3), 1.25 (s, 18H, C(CH_3)$_3$), 0.07 (s, 12 H, Ga(CH_3)$_2$); ^{13}C{^{1}H} NMR (benzene-d_6, 23 °C, ppm) 162.20 (s, *C*-C(CH_3)$_3$), 102.13 (s, pz ring *C*H), 50.21 (s, GaO*C*H$_3$), 32.05 (s, *C*(CH_3)$_3$), 31.22 (s, C(*C*H_3)$_3$), −4.61 (s, Ga(*C*H_3)$_2$). Anal. Calcd for $C_{16}H_{34}Ga_2N_2O$: C, 46.88; H, 8.36; N, 6.83. Found: C, 47.02; H, 8.19; N, 6.60.

Kinetics Measurements for 1. A 5 mm NMR tube was charged with **1** (0.053 g, 0.085 mmol) and toluene-d_8 (0.80 mL) in a glovebox under argon and was sealed with a plastic cap. The tube was transferred to the 125 MHz NMR probe, and ^{13}C{^{1}H} NMR spectra were recorded between −30 and 30 °C. At −30 °C, ^{13}C{^{1}H} NMR resonances for the *ipso*-carbon of the bridging and terminal phenyl groups were observed as sharp signals at 157.48 and 146.17 ppm. Upon warming from −30 to 30 °C, these resonances gradually broadened, and at 30 °C two broad peaks were observed at 157.11 and 146.49 ppm. The dynamic process was modeled as an AB_4 exchange using the ^{13}C{^{1}H} resonance broadening for the *ipso*-carbon of the bridging and terminal phenyl groups using the program gNMR.[15] Virtually identical spectra were observed for a sample of **1** (0.026 g, 0.042 mmol) in toluene-d_8 (0.80 mL) in the same temperature range, suggesting that the observed kinetic event was intramolecular.

Kinetics Measurements for 2·C_7H_8. In a fashion similar to the kinetics measurements for **1**, a solution of **2**·C_7H_8 (0.071 g, 0.085 mmol) in toluene-d_8 (0.80 mL) was used to record ^{13}C-{^{1}H} NMR spectra between −25 and 20.6 °C. At −25 °C, sharp ^{13}C{^{1}H} NMR resonances for the *ipso*-carbon of the bridging and terminal phenyl groups were observed at 157.93 and 146.15 ppm. Upon warming from −25 to 20.6 °C, these resonances gradually broadened, and at 20.6 °C two broad

peaks were observed at 157.92 and 146.51 ppm. Virtually identical spectra were obtained for a sample of **2**·C_7H_8 (0.035 g, 0.042 mmol) in toluene-d_8 (0.80 mL) in the same temperature range.

Kinetics Measurements for 3. In a fashion similar to the kinetics measurements for **1**, a solution of **3** (0.060 g, 0.085 mmol) in toluene-d_8 (0.80 mL) was used to record $^{13}C\{^1H\}$ NMR spectra between −12 and 28 °C. At −12 °C, sharp $^{13}C\{^1H\}$ NMR resonances for the *ipso*-carbon of the bridging and terminal phenyl groups were observed at 158.33 and 147.97 ppm. Upon warming from −12 to 28 °C, these resonances gradually broadened, and at 28 °C two broad peaks were observed at 158.28 and 148.24 ppm. Virtually identical spectra were obtained for a sample of **3** (0.030 g, 0.042 mmol) in toluene-d_8 (0.80 mL) in the same temperature range.

Kinetics Measurements for 4·(C_6H_{14})$_{0.5}$. In a fashion similar to the kinetics measurements for **1**, a solution of **4**·(C_6H_{14})$_{0.5}$ (0.060 g, 0.072 mmol) in toluene-d_8 (0.80 mL) was used to record $^{13}C\{^1H\}$ NMR spectra between −30 and 4 °C. At −30 °C, $^{13}C\{^1H\}$ NMR resonances for the *ipso*-carbon of the bridging and terminal phenyl groups were observed as slightly broad and sharp signals at 153.63 and 151.49 ppm, respectively. Upon warming from −30 to 4 °C, these resonances gradually broadened, and at 4 °C only one broad peak was observed at 151.63 ppm.

Crystallographic Structural Determinations of 2·C_7H_8, 3·(C_6H_{14})$_{0.5}$, 4·(C_6H_{14})$_{0.5}$, 6, and 9. Diffraction data were measured on a Bruker *P4/CCD* diffractometer equipped with Mo radiation and a graphite monochromator at 298 K (**2**·C_7H_8, **3**, **4**·(C_6H_{14})$_{0.5}$, and **6**) or 213 K (**9**). The samples collected at 298 K were mounted in thin-walled glass capillaries under an inert atmosphere. A sphere of data was measured at 10 s/frame and 0.2° between frames. The frame data were indexed and integrated with the manufacturer's *SMART* software.[19] All structures were refined using Sheldrick's *SHELX-97* software.[20]

Complex **2**·(C_7H_8) crystallized as colorless rhomboids. A crystal with dimensions of 0.2 × 0.1 × 0.02 mm^{-3} was used for data collection; 2450 frames were collected, yielding 15 404 reflections, of which 9789 were independent. Hydrogen positions were calculated. The neutral complex crystallized with 1 equiv of toluene that was disordered about a crystallographic inversion center. The disordered solvent was included in the calculations using Spek's *SQUEEZE* portion of the *PLATON* software suite.[21,22]

Complex **3**·(C_6H_{14})$_{0.5}$ crystallized as colorless flat rods, and a crystal with dimensions of 0.4 × 0.3 × 0.1 mm^{-3} was used for data collection; 2450 frames were collected, yielding 14 204 reflections, of which 9084 were independent. Hydrogen positions were observed or calculated. The asymmetric unit contains one neutral molecule and 1/2 hexane solvent disordered about an inversion center. The solvent exhibited large thermal parameters but was allowed to refine.

Complex **4**·(C_6H_{14})$_{0.5}$ crystallized as colorless rods, and a crystal with dimensions of 0.28 × 0.12 × 0.12 mm^{-3} was used for data collection; 2450 frames were collected, yielding 14 967 reflections, of which 9525 were independent. Hydrogen atoms were placed in calculated positions. The asymmetric unit consists of one neutral binuclear complex and 1/2 equiv of hexane solvent. The hexane occupies an inversion center.

Complex **6** crystallized as colorless rhomboids, and a crystal with dimensions of 0.2 × 0.2 × 0.2 mm^{-3} was used for data collection; 2450 frames were collected, yielding 15 988 reflections, of which 5322 were independent. Hydrogen positions were calculated. The asymmetric unit consists of one-half neutral binuclear complex occupying an inversion center.

Complex **9** crystallized as colorless flat rods, and a sample 0.6 × 0.4 × 0.1 mm^{-3} was used for data collection; 1850 frames were collected, yielding 10 160 reflections, of which 4508 were independent. Hydrogen positions were observed and refined, except those on C16 (methyl), which were calculated. The asymmetric unit consists of one neutral binuclear complex without solvent.

Acknowledgment. We are grateful to the National Science Foundation (CHE-9807269, Special Creativity Extension thereto, and CHE-0314615) for support of this research. Support for W.Z. came from the Office of Naval Research (grant no. N00014-21-0-866).

Supporting Information Available: X-ray crystallographic files in CIF format for the structure determinations of **2**·C_7H_8, **3**, **4**·(C_6H_{14})$_{0.5}$, **5**−**7**, and **9**. This material is available free of charge via the Internet at http://pubs.acs.org. Tables of kinetics data for **1**, **2**·C_7H_8, **3**, and **4**·(C_6H_{14})$_{0.5}$ are also available.

OM050623R

(19) *SMART, SAINT,* and *SADABS* collection and processing programs; Bruker AXS Inc.: Madison WI.

(20) Sheldrick, G. *SHELX-97*; University of Gottingen: Germany, 2003 and 1997.

(21) Spek, A. L. *PLATON*; Utrecht University: The Netherlands, 2003.

(22) Spek, A. L. *J. Appl. Crystallogr.* **2003**, *36*, 7.